Serum Amyloid A Binding to Formyl Peptide Receptor-Like 1 Induces Synovial Hyperplasia and Angiogenesis[1]

Mi-Sook Lee,* Seung-Ah Yoo,† Chul-Soo Cho,† Pann-Ghill Suh,* Wan-Uk Kim,[2†] and Sung Ho Ryu[2*]

Serum amyloid A (SAA) is a major acute-phase reactant, and has been demonstrated to mediate proinflammatory cellular responses. Although SAA has been used as an indicator for a variety of inflammatory diseases, the role of SAA in synovial hyperplasia and proliferation of endothelial cells, a pathological hallmark of rheumatoid arthritis (RA), has yet to be elucidated. In this study, we have demonstrated that SAA promotes the proliferation of human fibroblast-like synoviocytes (FLS). In addition, SAA protects RA FLS against the apoptotic death induced by serum starvation, anti-Fas IgM, and sodium nitroprusside. The activity of SAA appears to be mediated by the formyl peptide receptor-like 1 (FPRL1) receptor, as it was mimicked by the WKYMVm peptide, a specific ligand for FPRL1, but completely abrogated by down-regulating the FPRL1 transcripts with short interfering RNA. The effect of SAA on FLS hyperplasia was shown to be caused by an increase in the levels of intracellular calcium, as well as the activation of ERK and Akt, which resulted in an elevation in the expression of cyclin D1 and Bcl-2. Moreover, SAA stimulated the proliferation, migration, and tube formation of endothelial cells in vitro, and enhanced the sprouting activity of endothelial cells ex vivo and neovascularization in vivo. These observations indicate that the binding of SAA to FPRL1 may contribute to the destruction of bone and cartilage via the promotion of synoviocyte hyperplasia and angiogenesis, thus providing a potential target for the control of RA. *The Journal of Immunology,* **2006, 177: 5585–5594.**

Rheumatoid arthritis (RA)[3] is a multisystem autoimmune disease, which is characterized by chronic joint inflammation (1). The hallmark characteristics of RA pathology include the infiltration of inflammatory leukocytes, the proliferation of synovial cells, and the presence of extensive angiogenesis, which is also commonly referred to as rheumatoid pannus (2–4). Rheumatoid pannus is sometimes considered to be a local tumor. For example, synovial fibroblasts, the principal components of invading pannus, proliferate abnormally, resist apoptosis, and invade the local environment (5, 6). Synovial fibroblasts obtained from RA patients exhibited several oncogenes, including H-*ras* and p53, harboring somatic mutations (7, 8). They also abundantly express antiapoptotic proteins, including the FLICE inhibitory protein (9) and Bcl-2 (10), both of which exert protective effects against the apoptosis initiated via death receptor- or mitochondria-dependent pathways. Moreover, in a fashion similar to that of carcinogenesis, angiogenesis is considered to be a critical step in the progression of RA (4, 11–13).

Serum amyloid A (SAA) is a multifunctional apolipoprotein, 12- to 14-kDa in size. This protein is normally present in the bloodstream at a concentration of ~0.1 μM, but the concentration of SAA can increase up to 1000-fold within the first 24–36 h in response to a variety of injuries, including trauma, infection, inflammation, and neoplasia (14, 15). As with other acute-phase reactants, the liver is the primary site at which SAA production occurs, but the overproduction of SAA in extrahepatic areas has also been implicated in the pathogenesis of several chronic inflammatory diseases, including atherosclerosis, Alzheimer's disease, inflammatory arthritis, and several cancer variants (16, 17). Moreover, elevated SAA levels appear to be an important indicator for both the diagnosis and prognosis of chronic inflammatory diseases. For example, increased levels of SAA are frequently observed in the sera, synovial fluid, and inflamed synovium of RA patients, and these levels have been commonly used as highly sensitive markers for the disease activity of RA (18–20).

There are two known SAA receptors, including CD36 and LIMPII analogous-1 (CLA-1) (21) and lipoxin A_4 receptor/formyl peptide receptor-like 1 (FPRL1) (22, 23). FPRL1 is one of the classic chemoattractant receptors encompassing G protein-coupled seven transmembrane domains. Previous reports have pointed to a role for FPRL1 in the regulation of a variety of cellular responses in several cell types, including astrocytoma cell lines (24), neutrophils, monocytes, and T cells (25), as well as HUVECs (26). Recently, O'Hara et al. (27) showed that overexpressed SAA and FPRL1 in inflamed synovial tissue can be associated with the production of matrix metalloproteinase. However, it remains to be determined whether SAA and FPRL1 in the RA synovium are involved directly in the synovial proliferation and formation of an invading pannus. Furthermore, very little information is currently available regarding the intracellular pathway relevant to SAA signaling in RA synoviocytes.

*Division of Molecular Life Sciences, Pohang University of Science and Technology, Pohang, Korea; †Department of Internal Medicine, Catholic University of Korea, Seoul, Korea

Received for publication February 28, 2006. Accepted for publication August 2, 2006.

The costs of publication of this article were defrayed in part by the payment of page charges. This article must therefore be hereby marked *advertisement* in accordance with 18 U.S.C. Section 1734 solely to indicate this fact.

[1] This work was supported by a grant from the Ministry of Science and Technology/Korea Science and Engineering Foundation to the National Core Research Center for Systems Bio-Dynamics and the 21st Frontier Proteome Research of the Ministry of Science and Technology in the Republic of Korea.

[2] Address correspondence and reprint requests to Dr. Wan-Uk Kim, Department of Internal Medicine, Division of Rheumatology, School of Medicine, Catholic University of Korea, St. Vincent's Hospital, 93 Chi-Dong, Suwon 442-723, South Korea; E-mail address: wan725@catholic.ac.kr or Dr. Sung Ho Ryu, Division of Molecular Life Sciences, Pohang University of Science and Technology, Pohang 790-784, South Korea. E-mail address: sungho@postech.ac.kr

[3] Abbreviations used in this paper: RA, rheumatoid arthritis; SAA, serum amyloid A; FPRL1, formyl peptide receptor-like 1; OA, osteoarthritis; FLS, fibroblast-like synoviocyte; SNP, sodium nitroprusside; VEGF, vascular endothelial growth factor; siRNA, short interfering RNA; $[Ca^{2+}]_i$, intracellular Ca^{2+} concentration.

0022-1767/06/$02.00

In this study, we evaluated the role of SAA in synoviocyte hyperplasia and angiogenesis, as both processes are crucial and mutually complementary with regard to RA pathogenesis. We determined that SAA enhances the proliferation and survival of synovial fibroblasts via binding to its receptor, FPRL1, and that this effect is mediated by the activation of intracellular calcium, ERK, and Akt. Moreover, SAA appears to participate in neovascularization by increasing the proliferation, migration, tube formation, and sprouting activity of endothelial cells. Taken together, our data suggest that SAA may be directly involved in the destruction of bone and cartilage via the promotion of synoviocyte hyperplasia and angiogenesis, and thus may constitute a potential target for the treatment of RA.

Materials and Methods

Materials

Recombinant human SAA (endotoxin level < 0.1 ng/μg) was purchased from PeproTech. The amino acid sequence of recombinant human SAA corresponds to the sequence of human SAA 1α isotype except for addition of an N-terminal Met and substitution of Asp for Asn at position 60 and substitution of His to Arg at position 71. The synthetic peptide, WKYMVm was synthesized from Anygen A & Pep. All Abs used in this study were purchased from Cell Signaling Technology.

Isolation and culture of synovial fibroblasts and HUVECs

Fibroblast-like synoviocytes (FLS) were prepared from synovial samples obtained from patients with RA and osteoarthritis (OA), all of whom were also undergoing total joint replacement surgery. The FLS were isolated from the synovial tissues in accordance with a previously described procedure (28). In brief, fresh synovial tissues were minced into 2- to 3-mm pieces, then treated for 4 h with 4 mg/ml type I collagenase (Worthington Biochemical), and maintained in DMEM containing 10% FBS at 37°C in an atmosphere containing 5% CO_2. The cells were used at three to eight passages, during which time they evidenced a homogenous fibroblast population, and also exhibited a typical bipolar configuration, as observed under inverse microscopy. HUVECs were isolated from fresh human umbilical cords via collagenase (Worthington Biochemical) digestion, and then maintained in 20% FBS-containing M-199 medium, as previously described. All HUVECs were used after no more than five passages.

Cell proliferation assay

The RA FLS, OA FLS, and HUVECs were plated onto 24-well culture dishes at a density of 2×10^4 cells/well, and then permitted to attach overnight. After 24 h of serum starvation, the cells were treated for 72 h with a variety of mitogens. [^{3}H]Thymidine (1 μCi) was added to each of the wells before the final 6 h of incubation (29). Cell growth was also evaluated by counting the viable cells. Control and mitogen-treated cells were harvested by trypsinization, and the number of cells was determined with a hemocytometer, under $\times$100 magnification.

Apoptosis assay

Synoviocyte apoptosis was induced by 3 days of serum deprivation, or by treating the cells for 12 h with either sodium nitroprusside (SNP, 0.7 mM) or anti-Fas IgM (0.7 μg/ml) plus cyclohexamide (1 μg/ml). The degree of apoptosis was then evaluated by MTT assay and ELISA for DNA fragmentation. In the MTT assay, FLS were seeded in 24-well culture plates at a density of 2×10^4 cells/well. After 72 h of incubation with SAA or media alone, MTT solution was added to each of the wells, and then incubated for 2 h. The reaction was halted via the removal of MTT. Thereafter, DMSO (200 μl) was added to solubilize the formazan crystals. The plates were then subjected to 5 min of gentle shaking to ensure that the crystals had dissolved completely, and the absorbance was read at 540 nm with a microplate reader. The cellular DNA fragmentation assay was conducted using an ELISA kit (Roche Applied Science), based on the quantitative sandwich ELISA principle, using two mouse mAbs targeted against DNA and BrdU, as previously described (30). In brief, the BrdU-labeled DNA fragments of the samples were bound to the immobilized anti-DNA Ab, fixing it within the wells of a microtiter plate. The immune-complexed BrdU-labeled DNA fragments were then denatured and fixed to the surfaces of the plates via the application of microwave irradiation. In the final step, the anti-BrdU peroxidase conjugate was allowed to react with the BrdU that had been incorporated into the DNA. After the removal of the unbound peroxidase conjugates, the quantity of peroxidase bound within the immune complex was determined photometrically, using tetramethylbenzidine as a substrate.

Generation and transfection of short interfering RNA (siRNA) for FPRL1 transcripts

To down-regulate the FPRL1 transcripts using siRNA, the following target sequence was used: ^{300}AAU UCA CAU CGU GGU GGA CAU^{320}. The results of a BLAST search of siRNA sequence revealed no significant homology to any other sequences stored in the database. This oligonucleotide yielded comparable results. RA FLS were used in the siRNA transfection procedure (31). These cells were transfected with a final concentration of 20 nM FPRL1 siRNA or luciferase siRNA, as a control, using Lipofectamine reagent (Invitrogen Life Technologies) in accordance with the manufacturer's instructions. The cells were washed with serum-free medium and then incubated with transfection mixture for 4 h and 30 min, after which medium containing 10% FBS was added. The cells were collected after 24, 48, and 72 h of incubation, after which the levels of FPRL1 expression were determined via Northern blot analysis and ligand binding assay.

Northern blot analysis

The total RNA from the transfected RA FLS cells was isolated using a commercially available TRI reagent (Molecular Research Center), in accordance with the manufacturer's instructions. RNA samples (20 μg/lane) were electrophoresed on 1% agarose gels containing formaldehyde, transferred to Hybond-N membrane (Amersham Biosciences), immobilized with UV light and then hybridized with FPRL1 or actin probes labeled with biotin using the PCR DNA biotinylation kit (Kirkegaard & Perry Laboratories). The membranes were washed in prehybridization buffer with denatured 10 mg/ml carrier DNA (Sigma-Aldrich) at 42°C for 1 h. The denatured probe was then added into the buffer and incubated at 42°C overnight. The membranes were washed, incubated with detector block solution for 45 min, and then incubated with alkaline phosphatase-labeled streptavidin for 30 min. The membranes were washed again, and incubated with CDP-Star Chemiluminescent (Kirkegaard & Perry Laboratories). X-ray film was exposed to the membranes with intensifying screens and then developed.

Ligand binding assay

Ligand binding assay was performed as previously described (32). Briefly, RA FLS and OA FLS were seeded at 1×10^5 cells/well onto a 24-well plate and cultured overnight. After blocking them with blocking buffer (33 mM HEPES (pH 7.5), 0.1% BSA in DMEM) for 2 h, 500 pM of ^{125}I-labeled WKYMVm (Amersham Biosciences) was added to the cells in binding buffer (PBS containing 0.1% BSA), in the presence or absence of unlabeled WRWWWW (WKYMVm competitor for FPRL1 binding) (32), and incubated for 3 h at 4°C with continuous shaking. The samples were then washed five times with ice-cold binding buffer, and 200 μl of lysis buffer (20 mM Tris (pH 7.5) and 1% Triton X-100) was added to each well. After 20 min at room temperature, the lysates were collected and counted using a gamma ray counter.

ELISA for SAA

Synovial fluid of 10 RA patients with joint effusions was collected by arthrocentesis, as previously described (33). The concentration of human SAA in RA synovial fluid was measured by ELISA kit (BioSource International), according to the manufacturer's instruction.

Intracellular Ca^{2+} measurement

The isolated FLS were incubated with fluo-3-AM working solution (Molecular Probes) (34), containing 0.03% plutonic F-127 (the final concentration of fluo-3-AM was 20 μM/L) for 1 h at 37°C. After incubation, fluo-3-AM fluorescence in the cells was elicited at 488 nm with a high-power Ar^+ laser, and the emission bands were detected at 530 nm with a photomultiplier. The fluorescence signal was detected using a confocal laser scanning system (Lasersharp MRA2; Bio-Rad), equipped with a Nikon E-600 Eclipse microscope. The fluorescence intensity was measured both before (F_0) and after (F) the addition of SAA or PMA. The change in intracellular Ca^{2+} concentration $[Ca^{2+}]_i$ was expressed in terms of the F/F_0 ratio. A total of 50–120 images were scanned in each cell.

Western blot analysis

RA FLS were incubated for 24 h in DMEM without FBS, and then SAA (3 μM) was added to the cells for the indicated times. The treated RA FLS were then washed twice in PBS, dissolved in sample buffer (50 mM Tris-HCl, 100 mM NaCl, 0.1% SDS, 1% Nonidet P-40, 50 mM NaF, 1 mM

Na_3VO_4, 1 μg/ml aprotinin, 1 μg/ml pepstatin, and 1 μg/ml leupeptin), boiled, separated via SDS-PAGE, and transferred to nitrocellulose membranes. After immunoblot analysis with phospho-ERK1/2 (Thr^{202}/Tyr^{204}), phospho-Akt (Ser^{473}), phospho-STAT3 (Tyr^{705}), cyclin D1, or Bcl-2 Abs, the membranes were stripped and reincubated with anti-ERK, Akt, STAT3, or β-actin Ab, respectively, to detect total protein amounts.

Wounding migration and tube formation assay

The wounding migration and tube formation activity of the HUVECs were measured as previously described (35, 36). In brief, HUVECs plated at confluence on 60-mm culture dishes were wounded with pipette tips, then treated with SAA (0–5 μg/ml), WKYMVm (10 nM), or vascular endothelial growth factor (VEGF, 20 ng/ml) in M-199 medium, supplemented with 1% serum and 1 mM thymidine. After 12 h of incubation, migration was quantitated by counting the cells that moved beyond the reference line. For the tube formation assay, the HUVECs were seeded on a layer of previously polymerized Matrigel (BD Biosciences) with SAA (5 μg/ml), WKYMVm peptide (10 nM), a specific ligand for FPRL1 (37, 38) or VEGF (20 ng/ml). After 18 h of incubation, the cell morphology was visualized via phase-contrast microscopy and photographed. The degree of tube formation was quantified by measuring the length of tubes in five randomly chosen low-power fields (magnification, ×40) from each well using the image-Pro Plus v4.5 (Media Cybernetics).

Rat aorta ring assay

Aortas from male Sprague-Dawley rats were cross-sectioned into rings, and mounted onto polymerized Matrigel dishes (39). Matrigel (150 μl) was then positioned on top and allowed to gel. After 7 days, the aortic rings, incubated with PBS, SAA (3 and 5 μg/ml), WKYMVm (10 nM), VEGF (20 ng/ml), or FBS (10%) were analyzed under an inverted microscope.

Mouse Matrigel plug assay

C57BL/6 mice (7 wk of age) were given s.c. injections of 500 μl of Matrigel (40) containing PBS, SAA (80 μg), or WKYMVm (1 μg). After 7 days, the skins of the mice were pulled back to expose the Matrigel plugs, which remained intact. After the noting and photographing of any quantitative differences, hemoglobin levels were measured by the Drabkin method, using a Drabkin reagent kit 525 (Sigma-Aldrich) for the quantitative assessment of blood vessel formation. The hemoglobin concentration was calculated from the parallel assay of a known amount of hemoglobin. The Matrigel plugs were fixed in 4% formalin, embedded with paraffin, and stained using H&E.

Statistical analysis

All data are expressed as the mean ± SD from several separate experiments. Statistical comparisons were conducted via Student's t test, and a value for $p < 0.05$ was considered statistically significant.

Results

SAA stimulates synoviocyte proliferation

Synovial hyperplasia is one of the hallmarks of RA pathology (3, 41). Several studies have shown that RA FLS tend to divide at a more rapid rate than do synoviocytes obtained from normal or osteoarthritic joints (42). Therefore, we have attempted to determine whether SAA accelerates the proliferation of FLS acquired from both RA and OA patients by [^{3}H]thymidine incorporation assays. When the FLS were stimulated with 5 μM SAA for 1–5 days, the DNA synthesis activities of RA FLS and OA FLS were peaked at 3 days (Fig. 1*A*). Therefore, we treated 0.1–5 μM SAA for 3 days to RA FLS and OA FLS to check the dose dependency of SAA on FLS proliferation. As a result, the incorporation rate of [^{3}H]thymidine was increased in a dose-dependent fashion, with the maximal effect being detected at a SAA concentration of 5 μM (Fig. 1*B*). The numbers of RA FLS and OA FLS were also dose-dependently increased as the result of SAA treatment (Fig. 1, *C* and *D*), and this effect was greater for the RA FLS than for the OA FLS (Fig. 1*C*). Moreover, when the synovial fluid of different RA patients ($n = 10$) was added to RA FLS, the FLS proliferation was correlated well with the concentration of SAA in the synovial fluid ($r = 0.733$, $p = 0.016$). These results suggest that SAA is capable

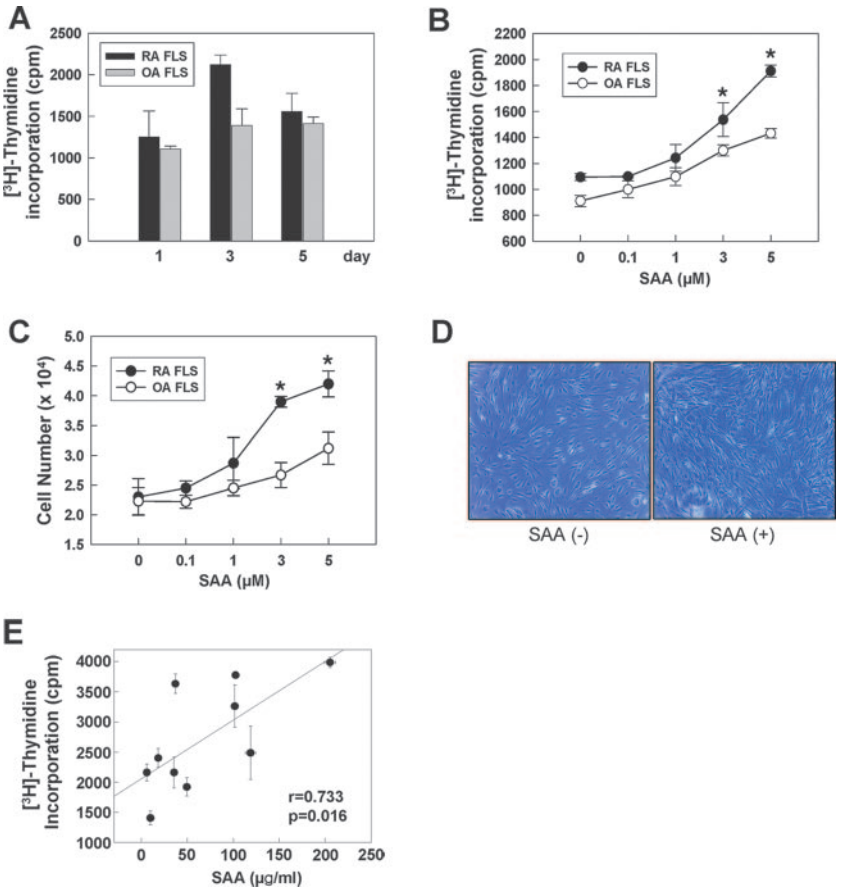

FIGURE 1. Proliferative effect of SAA on FLS. Primary cultured RA FLS and OA FLS were plated in triplicate, and [^{3}H]thymidine incorporation was used in the measurement of DNA synthesis activity in the presence of human recombinant SAA (5 μM) for 1, 3, or 5 days (*A*) and SAA (0, 0.1, 1, 3, or 5 μM) for 72 h (*B*). *C*, After 72 h of incubation with increasing doses of SAA (0, 0.1, 1, 3, or 5 μM), the RA FLS and OA FLS were trypsinized, and the cell numbers per well were determined under a microscope. The results are presented as the mean ± SD of three independent experiments using different cells from three different RA and OA patients. *, $p < 0.05$ vs the [^{3}H]thymidine incorporation (*B*) and cell number (*C*) of no treatment of SAA. *D*, RA FLS incubated in the presence or absence of 5 μM SAA for 72 h were photographed. Original magnification, ×50. *E*, SAA concentration of synovial fluid from 10 different RA patients was measured using SAA ELISA and the proliferative activity of RA FLS was evaluated after 72 h treatment of RA synovial fluid using [^{3}H]thymidine incorporation assay. Correlation between two variables was performed using Spearman's rank correlation coefficient.

of stimulating the abnormal proliferation of FLS, particularly in RA joints.

SAA protects rheumatoid synoviocytes from apoptotic death

Previous investigations have demonstrated a lack of apoptotic cells in RA FLS in the pannus, and this antiapoptotic characteristic appears to be required for FLS hyperplasia in RA (10, 43, 44). Therefore, we have attempted to determine the effects of SAA on FLS apoptosis. The viability of RA FLS and OA FLS was peaked at 3 days treatment of SAA (5 μM) (Fig. 2*A*). In addition, the treatment of RA FLS with SAA (0.1–5 μM) resulted in a dose-dependent inhibition of serum starvation-induced apoptosis, as determined by MTT assay and DNA fragmentation ELISA, as shown in Fig. 2, *B* and *C*. The antiapoptotic activity of SAA was shown to be more prominent in RA FLS than in OA FLS, a finding consistent with the data on SAA-induced synoviocyte proliferation (Fig. 1). In RA joints, the overproduction of NO as well as activated Fas signaling can induce apoptosis in the FLS (45–47). To simulate these conditions under in vitro conditions, we added SNP, a NO donor, or anti-Fas IgM Ab plus cycloheximide, to the cultured RA FLS. As had been expected, both SNP (0.7 mM) and anti-Fas (0.7 μg/ml) plus cycloheximide (1 μg/ml) resulted in a high level of DNA fragmentation in RA FLS, but this effect was blocked almost completely by cotreatment with SAA (3 μM) (Fig. 2, *D* and *E*). Together, our data appear to suggest that SAA is capable of rescuing RA FLS from apoptotic death in RA joints.

FPRL1 mediates SAA-induced proliferation and survival of synovial fibroblasts

FPRL1 has been identified as one of the receptors for SAA (22, 23, 27). Therefore, we assessed the levels of FPRL1 expression in RA FLS and OA FLS. As shown in Fig. 3*A*, FPRL1 mRNA was detected in most of the FLS, and was expressed more abundantly in RA FLS than in OA FLS. We also checked the expression level of FPRL1 displayed in the cellular membrane of RA FLS and OA FLS performing binding assay of ^{125}I-labeled WKYMVm, a specific ligand for FPRL1 (37, 48). Specific binding activity of ^{125}I-WKYMVm was higher in RA FLS than in OA FLS (21,538.1 $\pm$ 3,400.99 vs 15,830.2 $\pm$ 3,476.66, $p = 0.0015$), indicating the higher expression of FPRL1 protein in RA FLS than in OA FLS. These data suggest that RA FLS have a potential to respond more sensitively to FPRL1 ligation than OA FLS. We then attempted to determine the role of FPRL1 in the SAA-induced proliferation and survival of FLS. Because FPRL1-blocking Abs were commercially unavailable, WKYMVm peptide was used to stimulate FPRL1. As shown in Fig. 3*B*, the administration of the WKYMVm peptide induced a dose-dependent increase in the proliferation of RA FLS, but not OA FLS, whereas mitigating starvation-induced cell death. To verify that SAA activity is mediated by FPRL1 in the FLS, we conducted a blocking experiment using siRNA for FPRL1 transcripts. siRNA for luciferase and FPRL1 were designed, and were transiently transfected into RA FLS for 24–72 h. As is shown in

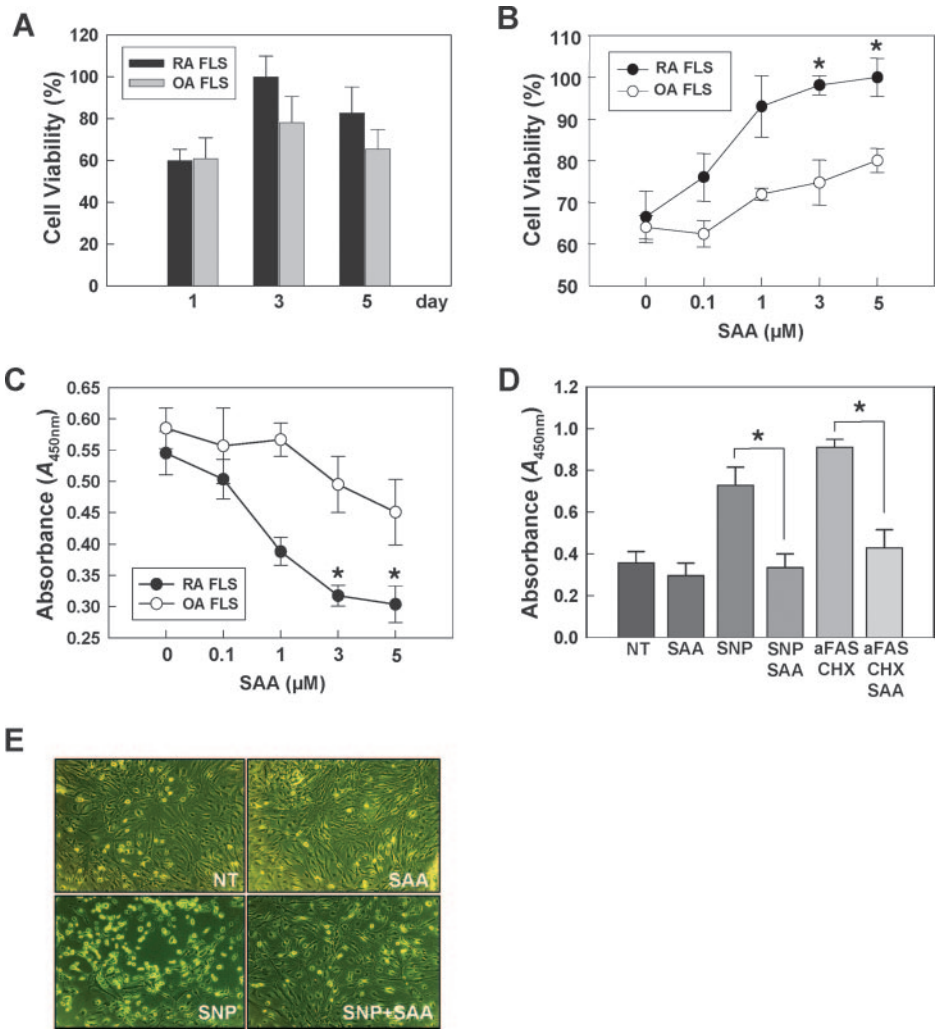

FIGURE 2. Increased viability of RA FLS by SAA treatment. In the MTT assay, RA FLS and OA FLS were treated with 5 μM SAA for 1, 3, and 5 days (*A*) and incubated with increasing concentrations of SAA (0–5 μM) for 72 h (*B*) under serum-deprived conditions. *, $p < 0.05$ vs the percentage of cell viability (%) of no treatment of SAA. *C*, Moreover, this antiapoptotic effect of SAA with increasing dose (0–5 μM) was detected again by measuring the levels of cellular DNA fragmentation under serum-deprivation conditions for 72 h. *, $p < 0.05$ vs the absorbance of no treatment of SAA. *D*, The levels of cellular DNA fragmentation of RA FLS induced by no treatment (NT), sodium nitroprusside (SNP, 0.7 mM) or IgM anti-FAS Ab (aFAS; 0.7 μg/ml) plus cycloheximide (CHX, 1.0 μg/ml) were measured in either the presence or absence of SAA (3 μM) for 12 h. *E*, Representative phase-contrast microscopy of RA FLS apoptosis was conducted 12 h after SNP treatment (0.7 mM) in the presence or absence of SAA (3 μM). NT, No treatment. Original magnification, $\times$50. Data are presented as the mean $\pm$ SD of three independent experiments using different cells from three different RA and OA patients.

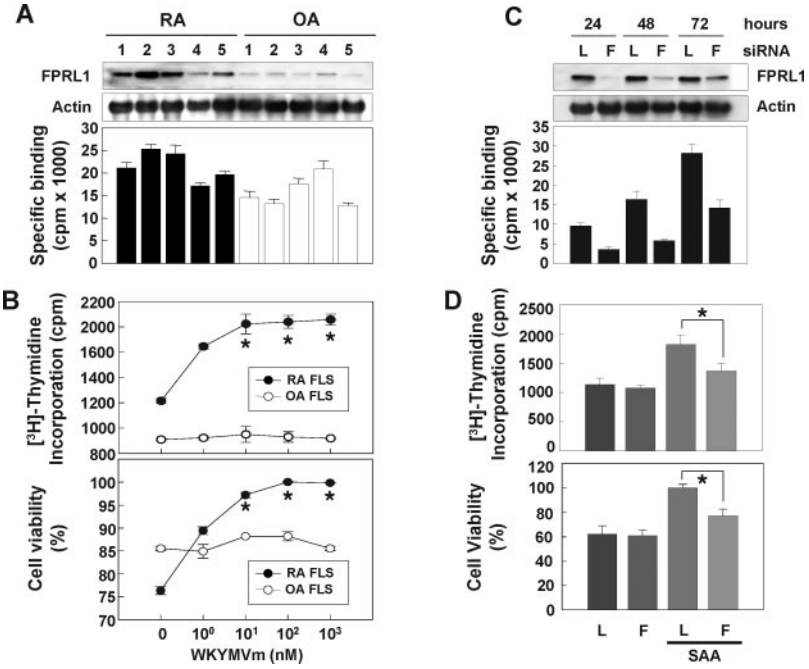

FIGURE 3. Increased proliferation and survival of RA FLS by SAA via FPRL1. *A*, FPRL1 mRNA expression levels and FPRL1 displayed at the cell membrane in the FLS obtained from five RA and five OA patients were analyzed by Northern blotting and ^{125}I-WKYMVm binding assay, respectively. FLS of each lane in blot corresponds to graph in binding assay (*bottom*). *B*, The specific agonist for FPRL1, WKYMVm peptide was added to the RA FLS and OA FLS in a concentration range from 1 to 1000 nM. After 72 h, the proliferative effects of WKYMVm were evaluated via a [^{3}H]thymidine incorporation assay, and the survival activity of WKYMVm was determined via an MTT assay. *, $p < 0.05$ in comparison with [^{3}H]thymidine incorporation (*top*) and viability (*bottom*) in the absence of WKYMVm. *C*, The down-regulation of FPRL1 mRNA by siRNA was established, and the mRNA and protein expression levels for FPRL1 were determined via Northern blot system and ^{125}I-WKYMVm binding assay after 24–72 h transfection. Luciferase (L) siRNA and FPRL1 (F) siRNA (target probe: 300–320) are shown. *D*, After 48 h of incubation of FPRL1 knock downed RA FLS in the absence or presence of SAA (5 μM), the degree of DNA synthesis (*top*) and apoptosis (*bottom*) was determined by [^{3}H]thymidine incorporation assay and DNA fragmentation ELISA, respectively. *, $p < 0.05$. Data are presented as the mean ± SD of two independent experiments using different cells from two different RA and OA patients.

Fig. 3*C*, the levels of FPRL1 mRNA expression were nearly completely abrogated 24 h after transfection of FPRL1 siRNA, and recovered 72 h after transfection. In contrast, there was no change for FPRL1 expression in cells transfected with luciferase siRNA as a control (Fig. 3*C*). The knockdown of FPRL1 mRNA in the FLS reduced the ability of SAA (5 μM) on the cell proliferation and survival (Fig. 3*D*), whereas siRNA for luciferase had no decreased effect on the proliferation and survival in the presence of SAA. Collectively, our results clearly indicate that FPRL1 is a major receptor, which mediates SAA-induced proliferation and the survival of RA FLS in the joints of RA patients.

SAA ligation to FPRL1 induces the release of intracellular Ca^{2+}

Our next experiment was conducted to evaluate the intracellular mechanisms inherent to effects of SAA on cellular proliferation and survival. Downstream events of FPRL1 activation are known to involve increases in intracellular Ca^{2+} (49), which is critical to virtually all cellular processes, including cell survival, proliferation, and death. Accordingly, the influence of SAA on Ca^{2+} release in FLS was thought to warrant careful consideration. Using a calcium-imaging system, we determined that the addition of SAA (3 μM) to RA FLS induced a 2.3-fold increase in intracellular Ca^{2+}, as compared with basal levels of Ca^{2+} (Fig. 4*A*). Moreover, the SAA-triggered release of Ca^{2+} was mimicked by the WKYMVm peptide (10 nM), and this increase was cancelled out by the pretreatment of cells with pertussis toxin (100 ng/ml), an antagonist of the G protein-coupled receptor (Fig. 4*B*), indicating that SAA may evoke a rise in $[Ca^{2+}]_i$ via FPRL1. It is noteworthy that RA FLS evidenced a higher degree of $[Ca^{2+}]_i$ release than did OA FLS, when stimulated with SAA, WKYMVm, or PMA (100 nM) (Fig. 4, *A* and *B*). This result shows that RA FLS harbors an intrinsic abnormality involving Ca^{2+} hyperresponsiveness to external stimuli, including SAA, and this abnormality may be associated with cellular hyperactivation.

ERK and Akt mediate the SAA-induced proliferation and survival of synoviocytes

Because ERK, Akt, and STAT3 activation are downstream targets of FPRL1 and are also critical for the proliferation and survival of several cell types, including RA FLS (50–52), we have attempted to determine whether SAA might induce the activation of ERK1/2, Akt, and STAT3 in RA FLS. RA FLS was shown to respond to 3 μM SAA with ERK1/2 and Akt phosphorylation, both of which proved detectable as early as 1 min after stimulation, and peaked at 1–5 min afterward (Fig. 5*A*, *upper panel*). SAA was also implicated in a gradual increase in STAT3 activation, which began to occur 5 min after incubation, and evidenced maximal phosphorylation levels at 30 min (Fig. 5*A*, *upper panel*). The SAA-induced increases in ERK and Akt phosphorylation were dose-dependent (Fig. 5*A*, *middle panel*). Moreover, both a dose- and time-dependent activation of ERK and Akt were noted in RA FLS stimulated with various concentrations of WKYMVm (1–1000 nM), an agonistic peptide for FPRL1 (Fig. 5*B*). Therefore, it appears that SAA may trigger an increase in the activation of ERK1/2, Akt, and STAT3 as well as $[Ca^{2+}]_i$ via the FPRL1 receptor, thereby promoting the proliferation and survival of synoviocytes. To address

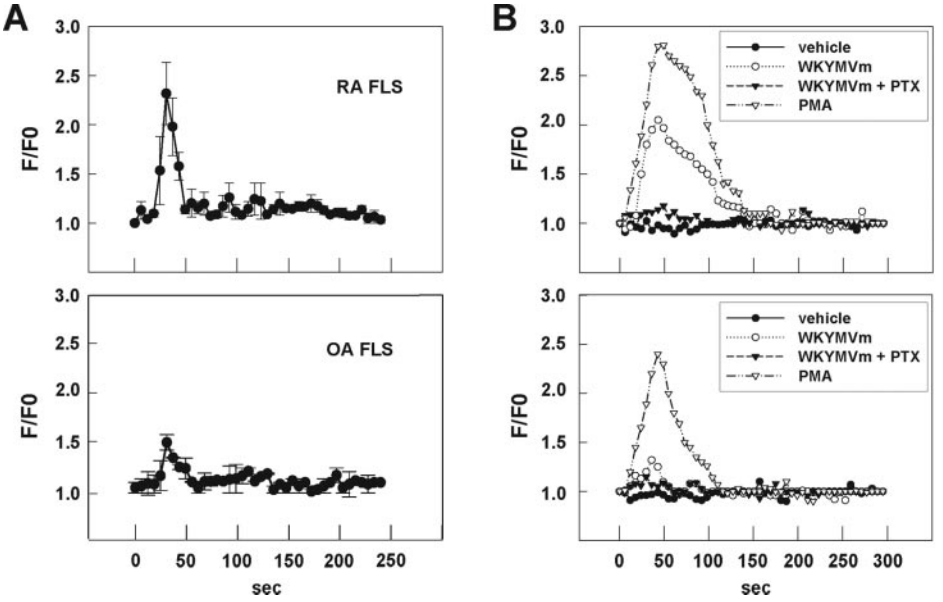

FIGURE 4. SAA-induced increase in $[Ca^{2+}]_i$ levels. Fluo-3-AM-loaded RA FLS and OA FLS were stimulated with SAA (3 μM) (*A*) and WKYMVm (10 nM) (*B*), an agonistic peptide for FPRL1, after which the relative levels of $[Ca^{2+}]_i$ were monitored with a calcium-imaging system. *B*, Pertussis toxin (PTX, 100 ng/ml) was administered to FLS for 12 h before the addition of WKYMVm. The results are presented as the mean ± SD of three independent experiments using different cells isolated from three different RA patients.

this hypothesis, we have conducted a series of blocking experiments using some pharmacological inhibitors of the described signaling molecules. As is shown in Fig. 5*C*, pretreatment of RA FLS with the G protein-coupled receptor inhibitor, PTX (100 ng/ml), the phospholipase C inhibitor U73122 (1 μM), the MEK inhibitor PD98059 (50 μM), or the PI3K inhibitor LY294002 (50 μM) for 1 h (6 h for pertussis toxin) resulted in the almost complete blockage of the proliferative and antiapoptotic activities of SAA. Collectively, our results show that the binding of SAA to FPRL1 facilitates the proliferation and survival of RA FLS via an increase in $[Ca^{2+}]_i$, as well as an enhancement of the activation of the ERK and Akt pathways.

The activation of the MAPK, ERK, and Akt, contributes to the maintenance of mitochondrial integrity, via the up-regulation of Bcl-2 expression (53). Based on our data regarding the survival advantage driven by SAA, we also examined the effects of SAA on cyclin D1 expression, which induces the transition of cells from G_1 arrest to the S phase, thereby leading to cell proliferation, as well as the expression of Bcl-2, a representative antiapoptotic molecule. When the RA FLS were treated with SAA (3 μM) or WKYMVm (10 nM) for various times, cyclin D1 expression increased significantly, exhibiting peak values as early as 4 h after treatment (Fig. 5, *A* and *B*, *lower panels*). The expression of Bcl-2 was also gradually elevated 8 h after stimulation with SAA or WKYMVm, and achieved peak levels between 12 and 24 h after stimulation (Fig. 5, *A* and *B*, *lower panels*). Collectively, our results suggest that SAA triggers the proliferation and survival of RA FLS, via the promotion of cyclin D1 and Bcl-2 expression.

SAA increases angiogenesis via the induction of endothelial proliferation, migration, tube formation, and sprouting activity

We finally attempted to determine whether SAA stimulates the proliferation of other types of FPRL1-harboring cells. As angiogenesis is considered to be a critical step in the progression of RA, and because HUVECs express FPRL1 on the surfaces of the cells, we assessed the proliferation activity of SAA in cultured HUVECs. As expected, SAA (0.1–5 μM) induced DNA synthesis in the HUVECs in a dose-dependent manner, with the maximum effects occurring at 5 μM. These effects were comparable to those generated in conjunction with the administration of 10 nM WKYMVm peptide and 20 ng/ml VEGF, a known mitogen in endothelial cells (Fig. 6*A*). Furthermore, the HUVECs treated with SAA (5 μM) evidenced concentration-dependent increases in migration from the edge of the wound into the open area (Fig. 6*B*). The migratory activity of the HUVECs stimulated with SAA (5 μM), WKYMVm (10 nM), or VEGF (20 ng/ml) was approximately three times higher than that of the control cells. We also examined the effects of SAA on the morphological differentiation of endothelial cells in the tube formation assay. Our findings indicated that the formation of elongated and robust tube-like structures was organized in a far superior fashion in the HUVECs treated with SAA (5 μM) than in the control HUVECs (Fig. 6*C*). To confirm the angiogenic potential of the SAA, the sprouting of endothelial cells from aortic rings, ex vivo and in vivo Matrigel plug angiogenesis trials were investigated in the presence of SAA. As can be seen in Fig. 6*D*, the sprouting of endothelial cells was increased as the result of SAA treatment, in a dose-dependent manner, whereas it was rarely observed in the absence of SAA. Moreover, the in vivo exposed Matrigel mixtures containing SAA (80 μg) or WKYMVm (1 μg) evidenced orange to red coloring, whereas the gels containing PBS retained their original white to amber coloring (Fig. 6*E*). In an attempt to quantify the angiogenesis in these samples, we measured the hemoglobin contents of the Matrigel mixture gels. The mean hemoglobin content of the SAA-treated Matrigels was 4.90 ± 0.66 g/dL, whereas the hemoglobin content of the PBS-contained gels was 0.53 ± 0.16 g/dL ($p < 0.05$). The stained sections indicated that Matrigels containing the SAA or WKYMVm peptide had produced more vessels in the gels than had the Matrigel containing the PBS (Fig. 6, *F–H*). These new vessels were filled with an abundance of intact RBC, indicating the formation of a functional vasculature within the Matrigels, and blood circulation in the newly formed vessels resulting from the angiogenesis induced by treatment with SAA or the WKYMVm peptide. Collectively, our results appear to suggest that SAA has potent angiogenic activity, under in vitro, ex vivo, and in vivo conditions.

Discussion

SAA has been implicated in a variety of chronic inflammatory diseases, including atherosclerosis, Alzheimer's disease, cancer, and RA. Prolonged or repeated inflammatory conditions, resulting in elevated SAA levels, can induce a reactive form of amyloidosis

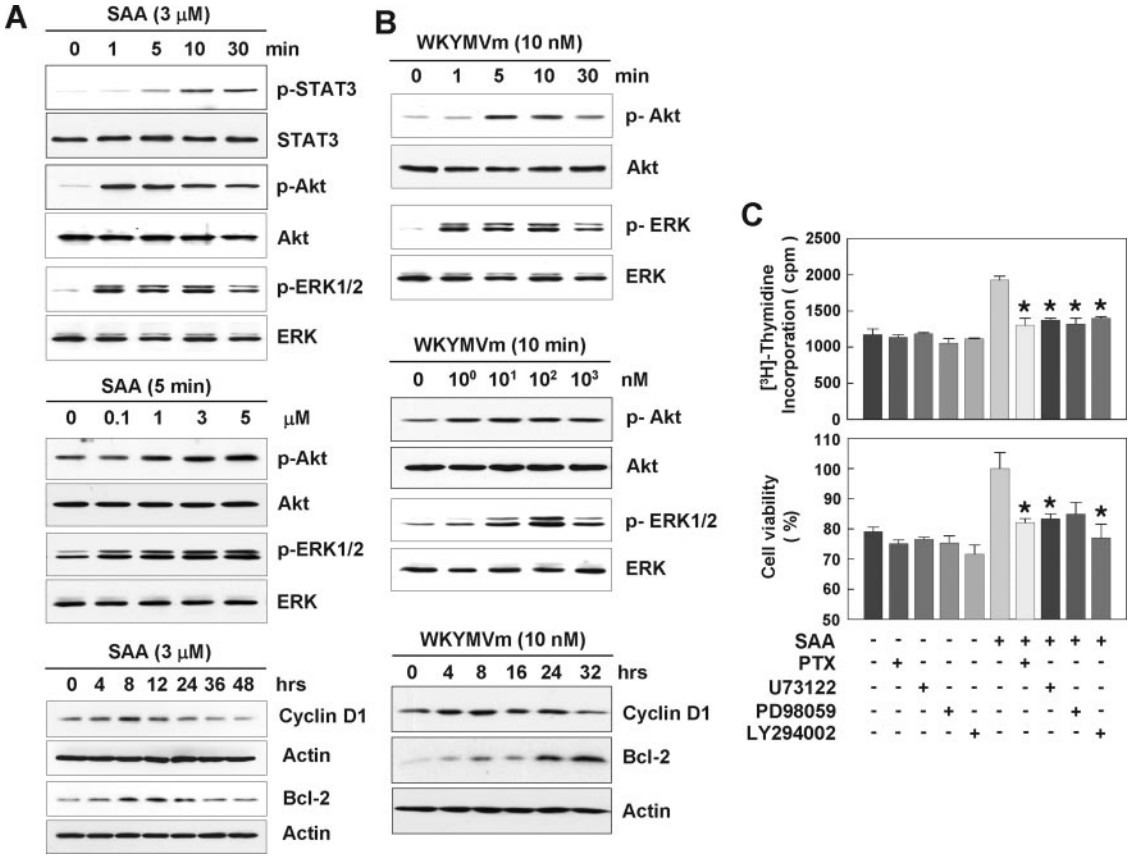

FIGURE 5. Activation of intracellular signaling molecules by SAA in RA FLS. RA FLS were incubated with 3 μM SAA (*A*) and 10 nM WKYMVm (*B*) for the indicated times, and ERK, Akt, and STAT3 phosphorylation were determined by Western blot analysis (*upper panels*). ERK and Akt activation were assessed after the application of treatment with the indicated amounts of SAA for 5 min and WKYMVm for 10 min (*middle panels*). RA FLS stimulated with SAA (3 μM) and WKYMVm (10 nM) were also subjected to Western blot analysis for cyclin D1 and Bcl-2 expression (*lower panels*). β-actin was used for the verification of equal protein loading in each lane. *C*, RA FLS were pretreated with pertussis toxin (PTX, 100 ng/ml), U73122 (1 μM), PD98059 (50 μM), or LY294002 (50 μM) before the addition of SAA (5 μM). After 72 h of incubation, the DNA synthesis (*top*) and survival (*bottom*) characteristics of the RA FLS were assessed by a [^{3}H]thymidine incorporation assay and an MTT assay, respectively. $*$, $p < 0.05$ in comparison with single treatment of SAA. Data are presented as mean $\pm$ SD of three independent experiments using three different RA FLS from RA patients with similar results.

in peripheral tissues, leading to progressive organ failure associated with amyloid accumulation (54). However, the findings of several recent studies have suggested that SAA may play a role in the inflammatory process as an active participant, rather than as a passive responder. For example, SAA may function as a chemoattractant for monocytes, polymorphonuclear leukocytes, mast cells, and T lymphocytes (23). SAA has been shown to stimulate the secretion of the proinflammatory cytokines, TNF-α and IL-1β, in both cultured human neutrophils and THP-1 monocytic cells (22, 54, 55). In the RA FLS, SAA has also been demonstrated to induce the secretion of both matrix metalloproteinase-1 and -3 (18, 19, 27). However, very little data are currently available regarding the functions of SAA in cellular proliferation and survival, as well as its intracellular targets.

In this study, we have shown that SAA stimulates the proliferation of FLS in vitro (Fig. 1). Moreover, SAA levels in RA synovial fluid were correlated well with proliferative activity of FLS, when RA FLS were treated with synovial fluid derived from 10 different RA patients (Fig. 1*E*). This observation suggests that excessive production of SAA in the joints could play a role in the pathogenesis of RA in vivo. SAA has also been shown to prevent RA FLS against the apoptotic death induced by serum starvation, SNP, or anti-Fas IgM (Fig. 2). SAA-induced increases in the proliferation and survival of FLS were mimicked by the FPRL1 specific ligand, WKYMVm (Fig. 3). The activity of SAA on the proliferation and survival of FLS appears to be mediated by FPRL1, as it was abrogated by down-regulating FPRL1 transcripts with siRNA (Fig. 3). SAA also increased the expression of cyclin D1 and Bcl-2 in rheumatoid synoviocytes (Fig. 5), which are critical for cell proliferation and survival, respectively, as well as the levels of phospho-ERK and phospho-Akt, both of which are located upstream of the cyclin D1 and Bcl-2 signaling pathways. Moreover, the proliferative and antiapoptotic activities of SAA were blocked completely by the treatment with pharmacological ERK and Akt inhibitors (Fig. 5). Collectively, these data indicate that the interaction between SAA and FPRL1 induces the proliferation and survival of rheumatoid synoviocytes, via the ERK and Akt pathways.

The results of this study also indicated that the ability of SAA to promote both cell proliferation and survival was higher in the RA FLS than in the OA FLS (Figs. 1 and 2), thereby suggesting that RA FLS is more susceptible to SAA stimulation. This hyperresponsiveness to SAA may be attributable to the increased expression of FPRL1 in the RA FLS, as compared with the OA FLS, as was observed in this study (Fig. 3*A*). It has also been reported that several proinflammatory cytokines, including TNF-α, IL-1β, and IL-6, up-regulate FPRL1 and SAA expression in RA FLS (27). Therefore, these cytokines may indirectly affect SAA response via

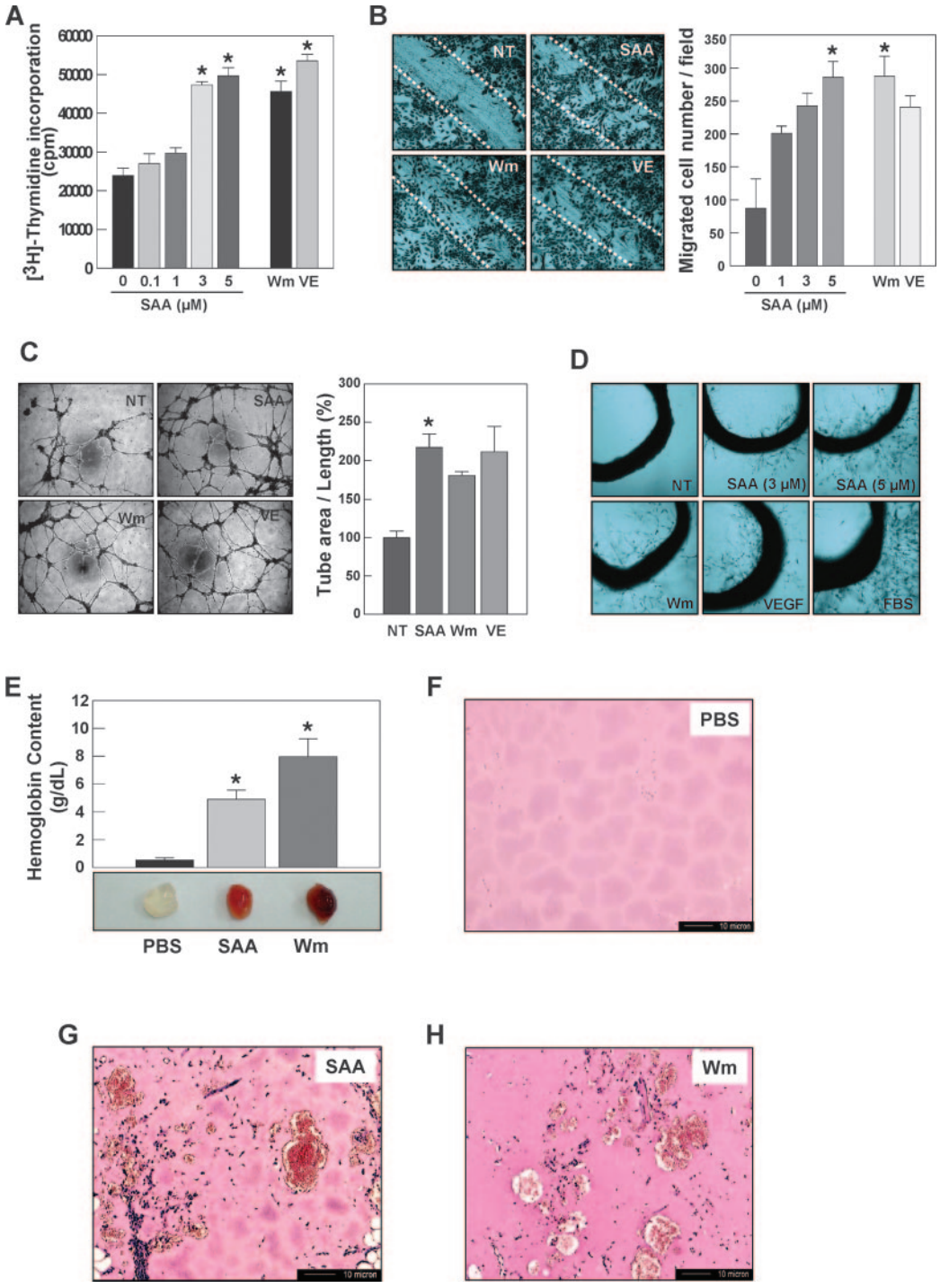

FIGURE 6. Effects of SAA on in vitro, ex vivo, and in vivo angiogenesis. The angiogenesis assays were conducted as described in *Materials and Methods*. *A*, The HUVECs were plated on M-199 supplemented with 20% serum. After 12 h of culture, different doses of SAA (0–5 μM), WKYMVm (10 nM), or VEGF (20 ng/ml) were added to M-199 medium supplemented with 1% serum. At 48 h, the amounts of DNA amount were determined via quantitation of the incorporated thymidine. Wm, WKYMVm; VE, VEGF. *B*, Confluent HUVECs were wounded with the tip of a micropipette, and incubated further in M-199 containing 1% serum with SAA (0–5 μM), WKYMVm (10 nM), or VEGF (20 ng/ml). After 12 h, the cells migrating beyond the reference line were photographed (magnification, $\times$50) and counted. *C*, The HUVECs were seeded on 48-wells precoated with Matrigel, and incubated in the presence of SAA (5 μM), WKYMVm (10 nM), or VEGF (20 ng/ml) for 18 h (original magnification, $\times$40). The degree of tube formation was quantified by measuring the length of tubes in five randomly chosen low-power fields from each well using the image-Pro Plus v4.5. NT, Not treated. $*$, $p < 0.05$ in comparison with no treatment of SAA (*A–C*). *D*, Rat aortic explants were incubated in M-199 harboring different dosages of SAA (3 and 5 μM), WKYMVm (Wm, 100 nM), VEGF (VE, 20 ng/ml), or 10% FBS. After 7 days, the ECs sprouting from the explants were photographed. Three independent experiments were then conducted, each in duplicate. NT, No treatment. *E–H*, C57BL/6 mice were injected s.c. with 0.5 ml of Matrigel supplemented with PBS, SAA (80 μg), or WKYMVm (Wm, 1 μg). After 7 days, the mice were sacrificed and the Matrigel plugs were excised and fixed. *E*, Representative Matrigel plugs containing PBS, SAA (80 μg), or WKYMVm (Wm, 1 μg) and the quantification of new vessel formation via measurements of the hemoglobin within the Matrigels are shown. Five mice were used for each group. Statistical comparisons were conducted by Student's *t* test. $*$, $p < 0.05$ vs the hemoglobin contents of the Matrigel containing PBS. *F–H*, Representative photograph shown of the gels shown in cross-section and stained with H&E. Original magnification, $\times$100. Data represent the mean $\pm$ SD, and similar results were obtained with two different experiments.

the up-regulation of FPRL1. Another possible explanation for the hyperresponsiveness might involve differences in the SAA-evoked signal transduction pathway between the RA FLS and OA FLS (Fig. 4). These increases in intracellular Ca^{2+} levels, as well as the activation of ERK and Akt, may more potently stimulate the expression of cyclin D1 and Bcl-2, resulting in enhanced proliferation and survival. Given the elevated SAA and FPRL1 expression levels in RA joints as compared with OA joints, the Ca^{2+} response and the activation of signaling molecules, most notably ERK and Akt, might be accentuated or further prolonged under in vivo arthritic conditions.

The supply of sufficient oxygen and nutrients via neovascularization is required for the perpetuation of synovial hyperplasia (4, 11). Furthermore, the newly formed blood vessels provide a surface to which leukocytes can adhere and through which they can migrate, delivering more inflammatory cells and molecules to arthritic lesions (12). Therefore, angiogenesis is essential to the progression of chronic arthritis, and also constitutes an early determinant of RA. Recently, Mullan et al. (56) demonstrated that SAA stimulates the migration of endothelial cells, leukocyte recruitment, and matrix degradation in RA. However, the functions of SAA in endothelial proliferation, as well as its in vivo effects on angiogenesis, remain to be clearly elucidated. In the present study, we determined that SAA stimulated proliferation, migration, and the formation of capillary tubes in vitro (Fig. 6). Moreover, the sprouting of endothelial cells was found to be up-regulated by SAA treatment in an ex vivo rat aorta sprouting assay (Fig. 6). The angiogenic activity of SAA was confirmed by the results of an in vivo mouse Matrigel plug assay (Fig. 6). Collectively, our findings, coupled with the findings of an earlier report (56), suggest that, in RA patients, SAA may facilitate the destruction of joints via the promotion of angiogenesis.

There are several potential mechanisms whereby SAA might exert positive effects on the survival characteristics of synoviocytes. First, as was suggested in this study, SAA, which is generated primarily by macrophages, endothelial cells, and synoviocytes, can exert an inhibitory effect on the apoptotic death of FLS, while inducing heightened cellular proliferation. Second, SAA may participate indirectly in the survival characteristics of synoviocytes, via the activation of inflammatory cascades. For example, SAA may recruit leukocytes in the synovial membrane (22, 55, 57), in which newly used leukocytes might induce the proliferation of synoviocytes via cell-to-cell contact. Thirdly, SAA promotes angiogenesis, which may diminish the growing burden of the synoviocytes, via the supply of oxygen and nutrients for tissue metabolism. As a result, expanded FLS might secrete elevated quantities of SAA, which would then further stimulate the proliferation of FLS in an autocrine or paracrine manner, thereby constructing a positive feedback loop. Taking these possibilities into account, SAA can be considered to be a critical mediator of pannus formation, and thus the development of an antagonist that would block the activity of SAA or FPRL1 might eventually prove useful with regard to the development of a treatment for RA. Such a possibility is currently under study and consideration.

In conclusion, SAA was shown to induce the proliferation of both FLS and endothelial cells, via its binding to its receptor, FPRL1. SAA was also shown to exert a protective effect against synoviocyte apoptosis. The cytoprotective and proliferative activity of SAA is achieved via the stimulation of intracellular Ca^{2+}, ERK, and Akt activity in the FLS. Our findings suggest that the interaction between SAA and FPRL1 may be critical to the hyperplasia of rheumatoid synoviocytes, and may also have important implications in terms of abnormal synoviocyte growth and therapeutic intervention in RA.

Disclosures

The authors have no financial conflict of interest.

References

1. Cornélis, F., S. Fauré, M. Martinez, J. F. Prud'homme, P. Fritz, C. Dib, H. Alves, P. Barrera, N. de Vries, A. Balsa, et al. 1998. New susceptibility locus for rheumatoid arthritis suggested by a genome-wide linkage study. *Proc. Natl. Acad. Sci. USA* 95: 10746–10750.
2. Kinne, R. W., R. Bräuer, B. Stuhlmüller, E. Palombo-Kinne, and G. R. Burmester. 2000. Macrophages in rheumatoid arthritis. *Arthritis Res.* 2: 189–202.
3. Pap, T., U. Müller-Ladner, R. E. Gay, and S. Gay. 2000. Fibroblast biology: role of synovial fibroblasts in the pathogenesis of rheumatoid arthritis. *Arthritis Res.* 5: 361–367.
4. Koch, A. E. 2003. Angiogenesis as a target in rheumatoid arthritis. *Ann. Rheum. Dis.* 62: ii60-ii67.
5. Feldmann, M., F. M. Brennan, and R. N. Maini. 1996. Rheumatoid arthritis. *Cell* 85: 307–310.
6. Firestein, G. S. 1996. Invasive fibroblast-like synoviocytes in rheumatoid arthritis. *Arthritis Rheum.* 39: 1781–1790.
7. Roivainen, A., J. Jalava, L. Pirila, T. Yli-Jama, H. Tiusanen, and P. Toivanen. 1997. H-*ras* oncogene point mutations in arthritic synovium. *Arthritis Rheum.* 40: 1636–1643.
8. Firestein, G. S., F. Echeverri, M. Yeo, N. J. Zvaifler, and D. R. Green. 1997. Somatic mutations in the p53 tumor suppressor gene in rheumatoid arthritis synovium. *Proc. Natl. Acad. Sci. USA* 94: 10895–10900.
9. Schedel, J., R. E. Gay, P. Kuenzler, C. Seemayer, B. Simmen, B. A. Michel, and S. Gay. 2002. FLICE-inhibitory protein expression in synovial fibroblasts and at sites of cartilage and bone erosion in rheumatoid arthritis. *Arthritis Rheum.* 46: 1512–1518.
10. Perlman, H., C. Georganas, L. J. Pagliari, A. E. Koch, K. Haines III, and R. M. Pope. 2000. Bcl-2 expression in synovial fibroblasts is essential for maintaining mitochondrial homeostasis and cell viability. *J. Immunol.* 164: 5227–5235.
11. Koch, A. E. 1998. Angiogenesis: implications for rheumatoid arthritis. *Arthritis Rheum.* 41: 951–962.
12. Kimball, E. S., and J. L. Gross. 1991. Angiogenesis in pannus formation. *Agents Actions* 34: 329–331.
13. Colville-Nash, P. R., and D. L. Scott. 1992. Angiogenesis and rheumatoid arthritis: pathogenic and therapeutic implications. *Ann. Rheum. Dis.* 51: 919–925.
14. Meek, R. L., and E. P. Benditt. 1986. Amyloid A gene family expression in different mouse tissues. *J. Exp. Med.* 164: 2006–2017.
15. Meek, R. L., S. Urieli-Shoval, and E. P. Benditt. 1994. Expression of apolipoprotein serum amyloid A mRNA in human atherosclerotic lesions and cultured vascular cells: implications for serum amyloid A function. *Proc. Natl. Acad. Sci. USA* 91: 3186–3190.
16. Jensen, L. E., and A. S. Whitehead. 1998. Regulation of serum amyloid A protein expression during the acute-phase response. *Biochem. J.* 334: 489–503.
17. Uhlar, C. M., and A. S. Whitehead. 1999. Serum amyloid A, the major vertebrate acute-phase reactant. *Eur. J. Biochem.* 265: 501–523.
18. Mitchell, T. I., C. I. Coon, and C. E. Brinckerhoff. 1991. Serum amyloid A (SAA3) produced by rabbit synovial fibroblasts treated with phorbol esters or interleukin 1 induces synthesis of collagenase and is neutralized with specific antiserum. *J. Clin. Invest.* 87: 1177–1185.
19. Vallon, R., F. Freuler, N. Desta-Tsedu, A. Robeva, J. Dawson, P. Wenner, P. Engelhardt, L. Boes, J. Schnyder, C. Tschopp, et al. 2001. Serum amyloid A (apoSAA) expression is up-regulated in rheumatoid arthritis and induces transcription of matrix metalloproteinases. *J. Immunol.* 166: 2801–2807.
20. Cunnane, G., S. Grehan, S. Geoghegan, C. McCormack, D. Shields, A. S. Whitehead, B. Bresnihan, and O. Fitzgerald. 2000. Serum amyloid A in the assessment of early inflammatory arthritis. *J. Rheumatol.* 27: 58–63.
21. Baranova, I. N., T. G. Vishnyakova, A. V. Bocharov, R. Kurlander, Z. Chen, M. L. Kimelman, A. T. Remaley, G. Csako, F. Thomas, T. L. Eggerman, and A. P. Patterson. 2005. Serum amyloid A binding to CLA-1 (CD36 and LIMPII analogous-1) mediates serum amyloid A protein-induced activation of ERK1/2 and p38 mitogen-activated protein kinases. *J. Biol. Chem.* 280: 8031–8040.
22. He, R., H. Sang, and R. D. Ye. 2003. Serum amyloid A induces IL-8 secretion through a G protein-coupled receptor, FPRL1/LXA4R. *Blood* 101: 1572–1581.
23. Su, S. B., W. Gong, J. L. Gao, W. Shen, P. M. Murphy, J. J. Oppenheim, and J. M. Wang. 1999. A seven-transmembrane, G protein-coupled receptor, FPRL1, mediates the chemotactic activity of serum amyloid A for human phagocytic cells. *J. Exp. Med.* 189: 395–402.
24. Le, Y., J. Hu, W. Gong, W. Shen, B. Li, N. M. Dunlop, D. O. Halverson, D. G. Blair, and J. M. Wang. 2000. Expression of functional formyl peptide receptors by human astrocytoma cell lines. *J. Neuroimmunol.* 111: 102–108.
25. De, Yang, Q. Chen, A. P. Schmidt, G. M. Anderson, J. M. Wang, J. Wooters, J. J. Oppenheim, and O. Chertov. 2000. LL-37, the neutrophil granule- and epithelial cell-derived cathelicidin, utilizes formyl peptide receptor-like 1 (FPRL1) as a receptor to chemoattract human peripheral blood neutrophils, monocytes, and T cells. *J. Exp. Med.* 192: 1069–1074.
26. Koczulla, R., G. von Degenfeld, C. Kupatt, F. Krötz, S. Zahler, T. Gloe, K. Issbrücker, P. Unterberger, M. Zaiou, C. Lebherz, et al. 2003. An angiogenic role for the human peptide antibiotic LL-37/hCAP-18. *J. Clin. Invest.* 111: 1665–1672.
27. O'Hara, R., E. P. Murphy, A. S. Whitehead, O. FitzGerald, and B. Bresnihan. 2004. Local expression of the serum amyloid A and formyl peptide receptor-like

1 genes in synovial tissue is associated with matrix metalloproteinase production in patients with inflammatory arthritis. *Arthritis Rheum.* 50: 1788–1799.
28. Yoo, S. A., D. G. Bae, J. W. Ryoo, H. R. Kim, G. S. Park, C. S. Cho, C. B. Chae, and W. U. Kim. 2005. Arginine-rich anti-vascular endothelial growth factor (anti-VEGF) hexapeptide inhibits collagen-induced arthritis and VEGF-stimulated productions of TNF-α and IL-6 by human monocytes. *J. Immunol.* 174: 5846–5855.
29. Guidoboni, M., P. Zancai, R. Cariati, S. Rizzo, C. J. Dal, A. Pavan, A. Gloghini, M. Spina, A. Cuneo, F. Pomponi, et al. 2005. Retinoic acid Inhibits the proliferative response induced by CD40 activation and Interleukin-4 in mantle cell lymphoma. *Cancer Res.* 65: 587–595.
30. Bauer, S., and P. H. Patterson. 2005. The cell cycle-apoptosis connection revisited in the adult brain. *J. Cell Biol.* 171: 641–650.
31. Sen, M., J. Reifert, L. Kevin, V. Wolf, J. S. Rubin, M. Corr, and D. A. Carson. 2002. Regulation of fibronectin and metalloproteinase expression by Wnt signaling in rheumatoid arthritis synoviocytes. *Arthritis Rheum.* 46: 2867–2877.
32. Bae, Y. S., H. Y. Lee, E. J. Jo, I. Kim, H. K. Kang, R. D. Ye, J. Y. Kwak, and S. H. Ryu. 2004. Identification of peptides that antagonize formyl peptide receptor-like 1-mediated signaling. *J. Immunol.* 173: 607–614.
33. Kim, W. U., S. Y. Min, M. L. Cho, J. Youn, J. K. Min, S. H. Lee, S. H. Park, C. S. Cho, and H. Y. Kim H. 2000. The role of IL-12 in inflammatory activity of patients with rheumatoid arthritis (RA). *Clin. Exp. Immunol.* 119: 175–181.
34. Harhun, M. I., D. V. Gordienko, O. V. Povstyan, R. F. Moss, and T. B. Bolton. 2004. Function of interstitial cells of Cajal in the rabbit portal vein. *Circ. Res.* 95: 619–626.
35. Lee, M. S., E. J. Moon, S. W. Lee, M. S. Kim, K. W. Kim, and Y. J. Kim. 2001. Angiogenic activity of pyruvic acid in in vivo and in vitro angiogenesis models. *Cancer Res.* 61: 3290–3293.
36. Kim, M. S., H. J. Kwon, Y. M. Lee, J. H. Baek, J. E. Jang, S. W. Lee, E. J. Moon, H. S. Kim, S. K. Lee, H. Y. Chung, et al. 2001. Histone deacetylases induce angiogenesis by negative regulation of tumor suppressor genes. *Nat. Med.* 7: 437–443.
37. Le, Y., W. Gong, B. Li, N. M. Dunlop, W. Shen, S. B. Su, R. D. Ye, and J. M. Wang. 1999. Utilization of two seven-transmembrane, G protein-coupled receptors, formyl peptide receptor-like 1 and formyl peptide receptor, by the synthetic hexapeptide WKYMVm for human phagocyte activation. *J. Immunol.* 163: 6777–6784.
38. Dahlgren, C., T. Christophe, F. Boulay, P. Madianos, M. J. Rabiet, and A. Karlson. 2000. The synthetic chemoattractant Trp-Lys-Tyr-Met-Val-DMet activates neutrophils preferentially through the lipoxin A_4 receptor. *Blood* 95: 1810–1818.
39. Sounni, N. E., L. Devy, A. Hajitou, F. Frankenne, C. Munaut, C. Gilles, C. Deroanne, E. W. Thompson, J. M. Foidart, and A. Noel. 2002. MT1-MMP expression promotes tumor growth and angiogenesis through an up-regulation of vascular endothelial growth factor expression. *FASEB J.* 16: 555–564.
40. Ferrari, N., U. Pfeffer, R. Dell'Eva, C. Ambrosini, D. M. Noonan, and A. Albini. 2005. The transforming growth factor-β family members bone morphogenetic protein-2 and macrophage inhibitory cytokine-1 as mediators of the antiangiogenic activity of *N*-(4-hydroxyphenyl)retinamide. *Clin. Cancer Res.* 11: 4610–4619.
41. Kramer, I., A. Wilulswas, K. Croft, and E. Genot. 2003. Rheumatoid arthritis: targeting the proliferative fibroblast. *Prog. Cell Cycle Res.* 5: 59–70.
42. Mohr, W., G. Beneke, and W. Mohing. 1975. Proliferation of synovial lining cells and fibroblasts. *Ann. Rheum. Dis.* 34: 219–224.
43. Matsmoto, S., U. Müller-Ladner, R. E. Gay, K. Nishioka, and S. Gay. 1996. Ultrastructural demonstration of apoptosis, Fas and Bcl-2 expression of rheumatoid synovial fibroblasts. *J. Rheumatol.* 23: 1345–1352.
44. Ceponis, A., J. Hietanen, M. Tamulaitiene, G. Partsch, H. Pätiälä, and Y. T. Konttinen. 1999. A comparative morphometric study of cell apoptosis in synovial membranes in psoriatic, reactive and rheumatoid arthritis. *Rheumtology* 38: 431–440.
45. Aupperle, K. R., D. L. Boyle, M. Hendrix, E. A. Seftor, N. J. Zvaifler, M. Barbosa, and G. S. Firestein. 1998. Regulation of synoviocytes proliferation, apoptosis, and invasion by the p53 tumor suppressor gene. *Am. J. Pathol.* 152: 1091–1098.
46. Borderie, D., P. Hilliquin, A. Hernvann, H. Lemarechal, C. J. Menkes, and O. G. Ekindjian. 1999. Apoptosis induced by nitric oxide is associated with nuclear p53 protein expression in cultured osteoarthritic synoviocytes. *Osteoarthritis Cartilage* 7: 203–213.
47. Santiago, B., M. Galindo, G. Palao, and J. L. Pablos. 2004. Intracellular regulation of Fas-induced apoptosis in human fibroblasts by extracellular factors and cycloheximide. *J. Immunol.* 172: 560–566.
48. Christophe, T., A. Karlsson, C. Dugave, M. J. Rabiet, F. Boulay, and C. Dahlgren. 2001. The synthetic peptide Trp-Lys-Tyr-Met-Val-Met-NH2 specifically activates neutrophils through FPRL1/lipoxin A_4 receptors and is an agonist for the orphan monocyte-expressed chemoattractant receptor FPRL2. *J. Biol. Chem.* 276: 21585–21593.
49. Hu, J. Y., Y. Le, W. Gong, N. M. Dunlop, J. L. Gao, P. M. Murphy, and J. M. Wang. 2001. Synthetic peptide MMK-1 is a highly specific chemotactic agonist for leukocyte FPRL1. *J. Leukocyte Biol.* 70: 155–161.
50. Rubinfeld, H., and R. Seger. 2005. The ERK cascade: a prototype of MAPK signaling. *Mol. Biotechnol.* 31: 151–174.
51. Krause, A., N. Scaletta, J. D. Ji, and L. B. Ivashkiv. 2002. Rheumatoid arthritis synoviocyte survival is dependent on Stat3. *J. Immunol.* 169: 6610–6616.
52. Morita, Y., N. Kashihara, M. Yamamura, H. Okamoto, S. Harada, and M. Kawashima. 1998. Antisense oligonucleotides targeting c-Fos m RNA inhibit rheumatoid synovial fibroblast proliferation. *Ann. Rheum. Dis.* 57: 122–124.
53. Pugazhenthi, S., A, Nesterova, C. Sable, K. A. Heidenreich, L. M. Boxer, L. E. Heasley, and J. E. Reusch. 2000. Akt/protein kinase B up-regulates Bcl-2 expression through cAMP-response element-binding protein. *J. Biol. Chem.* 275: 10761–10766.
54. Piirainen, H. I., A. T. Helve, T. Tornroth, and T. E. Pettersson. 1989. Amyloidosis in mixed connective tissue disease. *Scand. J. Rheumatol.* 18: 165–168.
55. Furlaneto, C. J., and A. Campa. 2000. A novel function of serum amyloid A: a potent stimulus for the release of tumor necrosis factor-α, interleukin-1β, and interleukin-8 by human blood neutrophil. *Biochem. Biophys. Res. Commun.* 268: 405–408.
56. Mullan, R. H., B. Bresnihan, L. Golden-Mason, T. Markham, R. O'hara, O. Fitzgerald, D. J. Veale, and U. Fearon. 2006. Acute-phase serum amyloid A stimulation of angiogenesis, leukocyte recruitment, and matrix degradation in rheumatoid arthritis through an NF-κB-dependent signal transduction pathway. *Arthritis Rheum.* 54: 105–114.
57. Patel, H., R. Fellowes, S. Coade, and P. Woo. 1998. Human serum amyloid A has cytokine-like properties. *Scand. J. Immunol.* 48: 410–418.